



Design and Fabrication of Deformable Microfluidic Device for the Study of Living Cells under Mechanical Solicitations

Naheed Hossain*, Zain Hayat and Abdel Illah El Abed

Laboratoire de photonique quantique et moléculaire, Ecole normale supérieure de Cachan, 94230 Cachan, Paris, France.

Received 15 June 2018; Received in revised form 25 November 2018

Accepted 08 January 2019; Available online 8 February 2019

ABSTRACT

Cellular symptoms present a model system for the analysis of living structures in laboratories such as metabolic studies and drug screening. In living organisms, cells are often encountered with compaction, tension, and shear. Most cells are intangible and balanced when a solid or seminal stratification (monolayer culture) is connected. In distortion reaction, cells experience intense biochemical changes. The stressed cells on the culture combine in the Vivo environment, which creates dramatic shape changes and biochemical reactions. These microsystems can meet broad applications in the biomedical research field since deformation, compression or fluid flow have been found to induce biochemical changes in cells derived from various tissues. The aim of this project is to design and to develop a microfluidic device which will allow for the culturing of adhered cells in microfluidic chambers (micro-wells) while controlling, at the micro scale, the mechanical deformation applied on the substrate on which cells are attached. During this work, a Polydimethylsiloxane (PDMS) double layered microfluidic device was designed and fabricated which enables controlled micro-sized deformation of the cell culturing microwells. Moreover, a relation was found between measured deformation values and simulations.

Keywords: MDA-MB-231; Micro-sized deformation; PDMS

1. Introduction

The work involved in this research was mainly inspired by the uprising success in the new research field of the so-called Organ-on-a-chip technology [1]. The state of art in the future development of this technology is envisioned not only by a complex “Human on a chip”, but also for a better understanding of tissue and cells *in vivo*. Organ-on-chip can replicate key functional units of living organs *in vitro* to reconstruct integrated human organ-level pathophysiology [2, 3]. These are the micro-engineered bio-mimetic micro-devices which can be used to test efficacy and toxicity of drugs and chemicals and to create *in vitro* models of human diseases. Organ-on-chip represents cost-effective alternatives to conventional animal models for pharmaceutical, chemical and environmental applications. For instance, there has been an increasing interest in the development of *in vitro* models of human intestinal functions, including cell culture systems that utilize trans-well filter which enable trans-epithelial barrier and transport studies and miniaturized microfluidic models that also support long-term culture [4, 5]. Most of the existing *in vitro* models do not recapitulate the mechanically active micro-environment of the human organ. By ceasing peristalsis-like motions while maintaining luminal flow, lack of epithelial deformation was shown to trigger bacterial overgrowth similar to that observed in patients with ileus and inflammatory bowel disease. The micro-system design incorporated multi-layers of closely apposed micro-fluidic channels separated by a thin porous membrane coated with ECM and lined by human epithelial cells enable analysis of epithelial barrier functions *in vitro* [6,7]. This device will allow for studying simultaneously cultured cells’ characteristics under different experimental conditions since cells will be confined in micro wells and trapped in isolated droplets. Epithelial cells will be cultured in the micro wells so that they can

face the mechanical solicitation under different environmental conditions. Two piston based united- vacuum chambers on both sides of the main cell-culturing channel with sufficient pressure allows us to produce the mechanical solicitation [8, 9]. This design of two layers stacked on top of another with a droplet-based system gives the opportunity to observe the development of epithelial cells. Two vacuum chambers on two sides can produce a different combination of pressure on the wells and mimic the proper mechanical solicitation on epithelial cells in the different parts of the human body. Micro-fluidic devices can facilitate the study of the mechanical regulation of human organs [10-12]. The novelty of the present work is inherent in droplet microfluidics. The existing work [1], [6] performed their experiments with the flow of biological fluidics. However, in this paper authors used the droplet technologies and anchoring techniques.

2. Methods

2.1 Background Physics

The force per unit length, f , to deform the wall of the vacuum chamber originates from the pressure difference ΔP across the width w of the chamber [13].

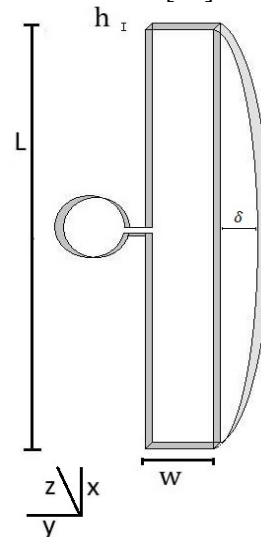


Fig. 1. Deformation of vacuum chamber due to the applied force.

For the height h of the vacuum chamber the deformation force per unit length, f is,

$$f = \Delta P h \quad (1)$$

It can be referred to the Euler-Bernoulli Eq. for the deformation of the vacuum chamber.

$$EI \left(\frac{d^4 v}{dy^4} \right) = f \quad (2)$$

In Fig. 1, L is the length of the vacuum chamber, W is the width; h refers to the height and δ refers to the maximum deformation. In Eq. 2, E is Young's modulus, I is the moment of inertia and v is the deformation. For a rectangular shaped vacuum chamber, the moment of inertia is found using Eq. 3.

$$I = \frac{W^3 h}{12} \quad (3)$$

2.2 Droplet Microfluidic

Microfluidics is an important and relatively new tool that emerged around 1975 and has found applications in many different scientific and technological areas. More specifically, droplet microfluidics technology allows for the production and manipulation at KHz rates of highly mono-disperse micro droplets, generally made of an aqueous solution dispersed in a continuous non-miscible inert carrier oil phase. The study of droplets formation has been an important field among other hydrodynamic instabilities. In this experiment flow focusing configuration is used which consists of two immiscible liquids that are injected together in a micro channel. Therefore, one of the liquids flows coaxially into the other, the central liquid breaks into drops when the capillary forces are bigger than the viscous forces, generating drops of equal sizes periodically emitted at the nozzle. The main problem in making mono-disperse droplets is the coalescence between them. The use of surfactants becomes essential in order to avoid this and make droplets easily. Surfactants are molecules formed by two parts, one hydrophobic and one hydrophilic. These molecules create a layer at the interface between the two immiscible liquids that prevent coalescing of the drop with

another one, even for high pressures. The use of surfactants affects the interface properties such as the surface tension [14].

3. Design

The fabricated microfluidic device consists of two stacked PDMS micro-patterned layers: 1) Cell-dispensing droplet generator layer. 2) A layer of wells. Fig. 2 shows the top view of two layers stacked microfluidic device. The cell-dispensing droplet generator has a chamber where drops form. These layers have two openings for the main chamber, one opening is used as an inlet and the other is used as an outlet. For mechanical solicitation, both of the layers have two vacuum chambers. Vacuum chambers and the main chamber have the equal length. They are used to make the mechanical solicitation respecting the piston law.

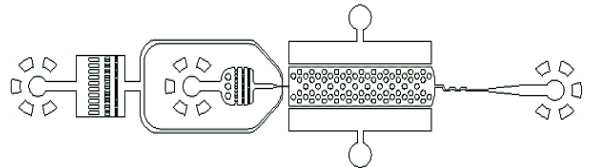


Fig. 2. Top view of two layers stacked microfluidic device.

The main device is comparable to 1 euro cent coin. Fig. 3 shows the main device inside the green rectangle. From Fig. 3 a comparison can be made between the length of the device and 1 euro cent coin (16.25mm diameter).

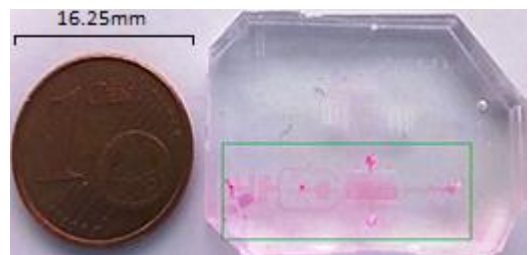


Fig. 3. Comparison between the length of the device and the diameter of 1 euro cent coin.

The gradual increment of pressure force in the range of 0 to 2000 millibar was introduced. The droplet generator can create mono-disperse droplets. The nozzle size is 100 μm and the average droplet size is in the range of 90 μm diameter. Because of the monodispersity property and for controlled droplets making facility, the flow focusing (FF) technique was chosen. In this technique one inlet is used to flow water and another inlet is used to flow oil. Droplets are made in a way like oil is cutting water. The membrane has 78 wells. These wells are distributed in a way that they follow the honeycomb structure. The honeycomb structure allows the membrane to reach the minimal weight and maximum strength. This structure provides relatively high compression properties and shear properties [15]. These layers have a common main chamber where cells can be cultivated. The mechanical solicitation makes deformation in the range of cell diameter [16].

4. Fabrication

4.1 Lithography

To make the mold, resin SU-8 (2075) was used. SU-8 (2075) gets polymerized when exposed to ultraviolet light [17]. To give resonance to the shape of the channel, it is necessary to use a mask, which was the negative image of the design. This mask is designed using a CAD software and then printed in a transparency sheet. High contrasts of masks are mandatory, especially for thick channels. The mold is fabricated by coating a thin layer of SU-8 on a silicon substrate which is soft baked to harden the resin; the resin stays 6 min at 65°C and then 3 min at 95°C [18]. Then the resin is exposed to UV light using the aligning machine MJB4 (in the clean room of “Le Laboratoire de photonique quantique et moléculaire (UMR 8537), École Normale supérieure Paris-Saclay”). MJB4 will also allow the alignment of two layers. Once the design is transferred, a second bake has to be done at the same temperatures before the developing process.

Two layers are required for this research work. For this purpose, the second layer of the same order is used in the first layer of the same level before the development process. Aligning marks according to the first and second layered designs were added to compare the second layer design with the first layer. To align the two designs, specific alignment marks were used on both layers. MJB4 was used to ensure the alignment of these two layers. Then the next process was to reveal the mold by a special SU-8 developer.

4.2 Molding, bonding and channel preparation

The Polydimethylsiloxane (PDMS) is a popular material used to fabricate microdevices; its properties make it highly suitable for almost any application [19]. It is optically transparent to wavelengths bigger than 280nm, which makes it perfect for this study, and it is convenient to use with cells and bacteria for potential applications. To make channels we mix a 10: 1 ratio of PDMS and the cross-linking agent was used. During the mix air bubbles are unavoidable. To take all the air out, the mix is introduced in a vacuum chamber until all the bubbles disappear. The mix then is poured into the mold that has been previously placed in an aluminium container. After pouring all the PDMS over the mold, some bubbles will appear, so it should wait some time until the air bubbles disappear. Once all bubbles have disappeared the PDMS is cured in a convective oven for 2 hours at 75°C [2]. When the curing time is over, the PDMS is cooled at room temperature, then it is cut into the desired shape to make the inlet and outlet holes. To close the channel, it should be meticulously cleaned using 3M “magic tape” to avoid any impurity during the bonding process. The channel is covered using a carefully cleaned microscope slide for one case. For other cases, the channel is covered using a cleaned slide of PDMS. The PDMS is attached to a microscope slide for the

second case. For the third case, the PDMS is not attached to a microscope slide. The two pieces are adhered using plasma bonding. The surface of the two pieces is activated using a ‘Harrick’ Plasma Cleaner chamber. This will change the surface, creating Si–OH groups on it which react with each other when the two surfaces are put in contact, creating a covalent link. Once the channels have been exposed to the plasma cleaner, the surface is no longer hydrophobic, so it is necessary to make some treatment to recover the hydrophobic proprieties of the PDMS and avoid the aqueous phase sticking to the walls. To make this, the channels were coated with silane [20]. (This process was done in the laboratory of ‘Le Laboratoire de photonique quantique et moléculaire (UMR 8537), École Normale supérieure Paris-Saclay”).

5. Simulation

The deflection of a well can be found by simulating the design in multi-physics simulation software. The design from CAD software was called in multi-physics simulation software. This design was transferred into three-dimensional versions.

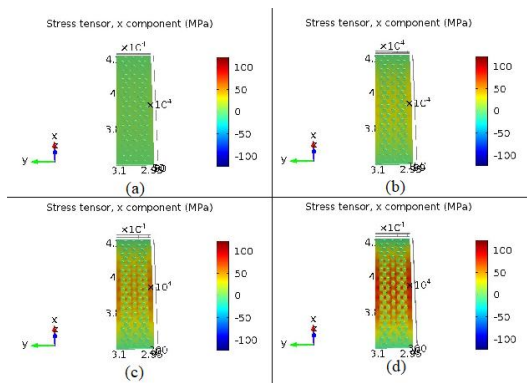


Fig. 4. Simulated deformation of wells under different pressure force applied. (a) 0mbar which was taken as the reference, (b) under 800mbar, (c) under 1600mbar,(d) simulated deformation of wells under 2000mbar.

With a proper multi-physics module, applied pressure force from 0millibar to 2000millibar with an increment of 200millibar was

considered on two sides of the membrane. Fig. 4 shows simulated deformation of wells under 0millibar, 800millibar, 1600millibar and 2000millibar. Fig. 5 shows the graph of simulated deformation of the wells along the x- axis under different pressure forces applied. In the case of simulation, the deformation of wells follows Eq. (5) and for the increment of 200millibar the deformation increases an average of 10um.

In simulation, the boundary condition on zero deflection and zero moment, $v(0) = 0$ and $v(L) = 0$.

$$y = 0, \left(\frac{d^2v}{dy^2}\right) = 0;$$

$$y = L, \left(\frac{d^2v}{dy^2}\right) = 0;$$

$$y = \frac{L}{2}, \left(\frac{d^2v}{dy^2}\right) = 0.$$

Integrating Eq. (2) with respect to y using boundary condition,

$$v(y) = \frac{L^3y - 2Ly^3 + y^4}{24EI} \tag{4}$$

Differentiating Eq. (4) and using boundary Eq. , we can also find the maximum deformation, δ

$$\delta = \frac{5PL^5}{384EI} \tag{5}$$

Considering, $K = \frac{5L^5}{384EI}$, in Eq. (5), $\delta = KP$. Here, maximum deformation is directly proportional to the applied pressure force.

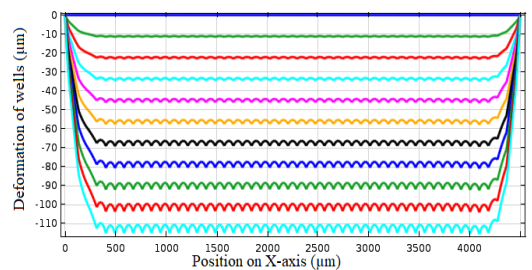


Fig. 5. Deformation of wells along X-axis.

6. Experimental Deformation

Fig. 6 shows the schematic diagram of the experimental setup. In the experiment, a program was used which allows incrementing the pressure after a specific amount of time. In order to find the best

deformation, three different approaches were used: (1) PDMS device sticking to the glass (2) PDMS device sticking to a thin layer of PDMS which is also sticking to the glass, and (3) PDMS device sticking to a thin layer of PDMS which is not sticking to the glass.

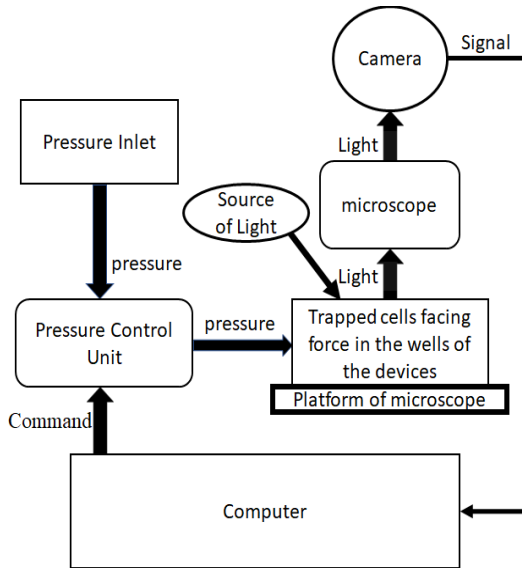


Fig. 6. Schematic diagram of the experimental setup.

In the case of approach (3), comparatively better deformations were achieved. Pressure force was applied in the range of 0 to 1800 millibar with the gradual increment to 200millibar. Deformation can be seen for 0millibar and 2000millibar in Fig. 7.

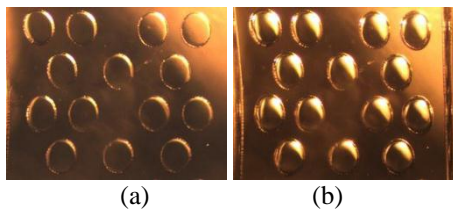


Fig. 7. Deformation of wells during experiment under pressure force applied. (a) 0millibar which was taken as reference (b) 2000millibar.

During the experiment, below 800millibar no deflection was found. Table 1 shows that the deformations are in μm range which is

equivalent to the diameter of the cell. Impulse and gradual increment of pressure force were applied for the minimum amount of time (sec). In both of the cases, threshold pressure forces were found. The threshold pressure force for impulse pressure force applied, P_T is much lower than threshold pressure force for the gradual increment pressure force applied, P_G .

Table 1. Deformation of well.

Pressure Force applied (millibar)	0	800	1600	2000
Deformation (μm)	0	3.721	6.082	10.162

7. Cell Culture

MDA-MB-231 cells were used in this experiment. The device was prepared by exposure to UV light for about 5min to activate the surface of the membrane. Then 4% of collagen (ECM) was applied for about 60 min. Phosphate Buffered Saline (PBS) or cell culture medium can be used to clean the device. During the cell culture, cells are bonded to the surface with antigen (protein) and when trypsin was applied, it breaks the bond. After cells started to flow, cells were placed for 4min in 37 C [21]. Then the cells were transferred in a plastic lab tube container.

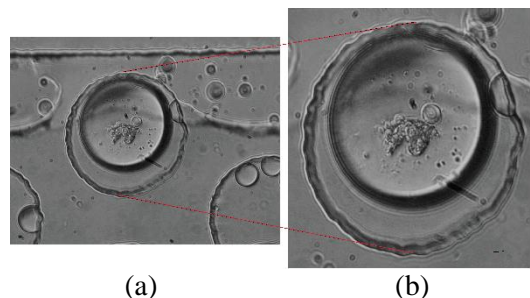


Fig. 8. (a) Anchored cells in well, (b) zoomed view of the droplet with cells in well.

The centrifugal force of about 100rpm was applied to the cells for 5 min. Then cells were found at the bottom of the plastic lab tube

[22-25]. Cells can be introduced with cell culture medium in the droplets with the help of a drop maker. Cells with cell culture medium can replace the disperse phase [26]. The oil phase will cut the cell culture medium and thus make droplets with cells. Poisson's Distribution Law can provide the number of cells in a droplet. Fig. 8 shows that the droplets were anchored to place the cells on the surface of the wells of the membrane. So apparently, cells are trapped in the wells to face mechanical solicitations. The gradient of surface energy and hydrodynamic drag anchors the droplet [27, 28]. Fluorinated oil has advantages of absorbing O₂ and CO₂. This will help to flow O₂ and CO₂ in wells that will help cells to live and grow in this environment.

8. Conclusion

The paper presents the development of the microfluidic device that can be helpful for a long range of biological study even including high throughput experiments. The paper describes the methodology for the construction of the presented device clearly. However, in real experiments deformation was multiple times smaller. According to Eq. (5), during small pressure changes, there should have been bigger deflection. However, mathematically deformation should be proportional to the applied pressure force. In experimental deformation, it is also found that after crossing the threshold pressure force the deformation is directly proportional to applied pressure. In the simulation, it is found that deformation also follows the direct proportionality with applied pressure. In the results, due to experimental limitations, the data is subjected to the error of (+/-)1 μm [29]. The application of droplet microfluidic and continuous phase flow with mechanically deformable 3D microfluidic chip allows making a deformation of approximately 10 μm. The use of fluorinated oil facilitates the growth of cells and a good living condition for them. The challenges in

microfluidic design with mechanical solicitation are the formation and adjustment of micro-droplets, trapping or anchoring the drops with cells and controlling the number of cells per drops. Using PDMS gives facilities such as optical stiffness, high gas permeability and, most importantly, biocompatibility [30]. Moreover, microfluidic production of droplets can be scaled up to a high throughput platform offering great potential for numerous applications in life and material science. The authors' future work will be devoted to testing the device with cells for a long period of time for various chemical solutions. This work is a beginning for building a device which can be used to prescribe the specific dose of medicine for an individual patient.

Acknowledgements

All these processes were done in the clean room and microfluidic laboratory of École Normale supérieure Paris-Saclay and l'Institut d'Alembert (IDA). Special thanks to "EU funded Erasmus+ program" for funding MONABIPHOT Master Students. Authors want to express heartfelt gratitude to Professor Isabelle Ledoux-Rak and Dr. Ngoc Diep Lai for their continuous support. Thanks to Dr. Rasta Ghasemi and Jean-Pierre Lefevre for sharing their experience. Special thanks to Professor Bruno Le Pioufle for his direction in the simulation part.

References

- [1] Bhatia SN, Ingber DE. Microfluidic organs-on-chips. *Nature biotechnology*. 2014 Aug;32(8):760.
- [2] Huh D, Kim HJ, Fraser JP, Shea DE, Khan M, Bahinski A, Hamilton GA, Ingber DE. Microfabrication of human organs-on-chips. *Nature protocols*. 2013 Nov;8(11):2135.
- [3] Xie S, Gardeniers JG, Luttge R. Nanoscale membrane actuator for in vitro mechano-stimuli responsive studies of neuronal cell networks on chip. *Journal of Micromechanics and Microengineering*. 2018 May 9;28(8):085011.

- [4] Bajaj P, Harris JF, Huang JH, Nath P, Iyer R. Advances and challenges in recapitulating human pulmonary systems: at the cusp of biology and materials. *ACS Biomaterials Science & Engineering*. 2016 Mar 14;2(4):473-88.
- [5] Blake AJ, Finger DS, Hardy VL, Ables ET. RNAi- Based Techniques for the Analysis of Gene Function in Drosophila Germline Stem Cells. *RNAi and Small Regulatory RNAs in Stem Cells: Methods and Protocols*. 2017:161-84.
- [6] Kim HJ, Li H, Collins JJ, Ingber DE. Contributions of microbiome and mechanical deformation to intestinal bacterial overgrowth and inflammation in a human gut-on-a-chip. *Proceedings of the National Academy of Sciences*. 2016 Jan 5;113(1):E7-15.
- [7] Li X, Valadez AV, Zuo P, Nie Z. Microfluidic 3D cell culture: potential application for tissue-based bioassays. *Bioanalysis*. 2012 Jun;4(12):1509-25.
- [8] Gonzalez-Andrades M, Alonso-Pastor L, Mauris J, Cruzat A, Dohlman CH, Argüeso P. Establishment of a novel in vitro model of stratified epithelial wound healing with barrier function. *Scientific reports*. 2016 Jan 13;6:19395.
- [9] Groschwitz KR, Hogan SP. Intestinal barrier function: molecular regulation and disease pathogenesis. *Journal of Allergy and Clinical Immunology*. 2009 Jul 1;124(1):3-20.
- [10] Williams JM, Duckworth CA, Burkitt MD, Watson AJ, Campbell BJ, Pritchard DM. Epithelial cell shedding and barrier function: a matter of life and death at the small intestinal villus tip. *Veterinary pathology*. 2015 May;52(3):445-55.
- [11] Sun X, Yang Q, Rogers CJ, Du M, Zhu MJ. AMPK improves gut epithelial differentiation and barrier function via regulating Cdx2 expression. *Cell death and differentiation*. 2017 May;24(5):819.
- [12] Sareen D, Saghizadeh M, Ornelas L, Winkler MA, Narwani K, Sahabian A, Funari VA, Tang J, Spurka L, Punj V, Maguen E. Differentiation of human limbal-derived induced pluripotent stem cells into limbal-like epithelium. *Stem Cells Translational Medicine*. 2014 Sep 1;3(9):1002-12.
- [13] Ashby MF. Materials selection in mechanical design. *MRS Bull*. 2005 Dec;30(12):995.
- [14] Gu H, Duits MH, Mugele F. Droplets formation and merging in two-phase flow microfluidics. *International journal of molecular sciences*. 2011 Apr 15;12(4):2572-97.
- [15] Li X, Liu H, Niu X, Yu B, Fan Y, Feng Q, Cui FZ, Watari F. The use of carbon nanotubes to induce osteogenic differentiation of human adipose-derived MSCs in vitro and ectopic bone formation in vivo. *Biomaterials*. 2012 Jun 1;33(19):4818-27.
- [16] Whitcutt MJ, Adler KB, Wu R. A biphasic chamber system for maintaining polarity of differentiation of culture respiratory tract epithelial cells. *In vitro cellular & developmental biology*. 1988 May 1;24(5):420-8.
- [17] Taylor AM, Dieterich DC, Ito HT, Kim SA, Schuman EM. Microfluidic local perfusion chambers for the visualization and manipulation of synapses. *Neuron*. 2010 Apr 15;66(1):57-68.
- [18] A del Campo and C Greiner 2007 *J. Micromech. Microeng.* 17 R81 [Internet]. [cited 2018 June 14]. Available from: <http://iopscience.iop.org/article/10.1088/0960-1317/17/6/R01/meta>
- [19] McDonald JC, Whitesides GM. Poly (dimethylsiloxane) as a material for fabricating microfluidic devices. *Accounts of chemical research*. 2002 Jul 16;35(7):491-9.
- [20] Patrito N, McLachlan JM, Faria SN, Chan J, Norton PR. A novel metal-protected plasma treatment for the robust bonding of polydimethylsiloxane. *Lab on a Chip*. 2007;7(12):1813-8.
- [21] Härmä V, Virtanen J, Mäkelä R, Happonen A, Mpindi JP, Knuutila M, Kohonen P, Lötjönen J, Kallioniemi O, Nees M. A comprehensive panel of three-dimensional models for studies of prostate cancer growth, invasion and drug responses. *PloS one*. 2010 May 3;5(5):e10431.
- [22] Hess MW, Pfaller K, Ebner HL, Beer B, Hekl D, Seppi T. 3D versus 2D cell culture: implications for electron

- microscopy. In *Methods in cell biology* 2010 Jan 1;96: 649-670.
- [23] Bergmann S, Steinert M. From single cells to engineered and explanted tissues: new perspectives in bacterial infection biology. In *International review of cell and molecular biology* 2015 Jan 1;319:1-44.
- [24] Marlene MarleneSchwanzel, Li Li-MouZheng, Hugo, Gary, Donald W. LHRH neurons: functions and development [Internet]. *Egyptian Journal of Medical Human Genetics*. Elsevier; 2008 [cited 2018Jun15]. Available from: <https://www.sciencedirect.com/science/article/pii/S0079612308645720?via=ihub>
- [25] Nathwani AC, Tuddenham EG, Rangarajan S, Rosales C, McIntosh J, Linch DC, Chowdary P, Riddell A, Pie AJ, Harrington C, O'beirne J. Adenovirus-associated virus vector– mediated gene transfer in hemophilia B. *New England Journal of Medicine*. 2011 Dec 22;365(25):2357-65.
- [26] Wang BL, Ghaderi A, Zhou H, Agresti J, Weitz DA, Fink GR, Stephanopoulos G. Microfluidic high-throughput culturing of single cells for selection based on extracellular metabolite production or consumption. *Nature biotechnology*. 2014 May;32(5):473.
- [27] Bjork SM, Sjostrom SL, Andersson-Svahn H, Joensson HN. Metabolite profiling of microfluidic cell culture conditions for droplet based screening. *Biomicrofluidics*. 2015 Jul;9(4):044128.
- [28] Alles J, Karaiskos N, Praktiknjo SD, Grosswendt S, Wahle P, Ruffault PL, Ayoub S, Schreyer L, Boltengagen A, Birchmeier C, Zinzen R. Cell fixation and preservation for droplet-based single-cell transcriptomics. *BMC biology*. 2017 Dec;15(1):44.
- [29] Moon S, Ceyhan E, Gurkan UA, Demirci U. Statistical modeling of single target cell encapsulation. *PLoS One*. 2011 Jul 21;6(7):e21580.
- [30] *Material Property Database, Material: PDMS (polydimethylsiloxane)* [Internet]. [cited 2018 June 14]. Available from: <http://www.mit.edu/~6.777/matprops/pdms.htm>